DEFORMATION PROPERTIES OF VERY LOOSE SAND IN UNDRAINED CYCLIC TORSIONAL SHEAR TESTS WITH INITIAL STATIC SHEAR

Muhammad UMAR[1], Gabriele CHIARO[2] and Takashi KIYOTA[3]

ABSTRACT: In this study, the effects of initial static shear on large deformation behavior of very loose (D_r =24-30%) Toyoura sand undergoing undrained cyclic loading was evaluated. To this scope, a series of torsional simple shear tests were carried out on hollow cylindrical specimens up to single amplitude shear strain exceeding 50%. Six isotopically consolidated specimens were subjected to reversal and non-reversal stress loading modes, depending on the superimposition of applied static and cyclic shear stresses. It was observed that, undrained soil strength, effective stress path and cyclic strain development were significantly influenced by the applied static shear and the imposed mode of loading. Moreover, it was confirmed that, similar to the case of loose Toyoura sand (D_r = 44-50%) previously investigated by the authors, also for very loose Toyoura sand, three failure mechanisms, namely cyclic liquefaction, rapid flow liquefaction and residual deformation, were observed. Under reversal stress conditions, full liquefaction (i.e. maximum generation of excess pore water pressure) took place beside rapid development of large deformation. On the contrary, in the case of no-reversal stress conditions, progressive accumulation of residual deformation brought the specimens to failure although full liquefaction state was not reached.

Key Words: *large strain, liquefaction, loose sand, static shear stress, torsional shear test*

INTRODUCTION

Liquefaction of saturated loose sandy deposits is a major cause for large ground deformations and catastrophic failure of foundations, natural slopes, embankments etc. during earthquakes. For example, disastrous slope failures due to liquefaction were observed during the 1964 Niigata, Japan, and the 1964 Great Alaskan Earthquakes, USA (Hamada et al., 1994). In 1971, the San Fernando earth-dam liquefied and collapsed during a powerful earthquake that hit Southern California, USA (Seed et al., 1975). More recently, during the 2010-2011 Canterbury Earthquake Sequence (New Zealand) and the 2011 Off the Pacific Coast of Tohoku Earthquake (Japan), extensive liquefaction-induced lateral spreading occurred in sloped ground and produced severe damage to residential houses and buildings, industrial and commercial structures, road and bridge infrastructures, lifeline facilities and levees (Cubrinovski et al. 2010, 2011; Kiyota et al., 2011; among others). Lateral spreading and liquefaction were also observed nearby a damaged earth dam-embankment following the 2015 Gorkha Nepal Earthquake (Chiaro et al., 2015).

The role of initial static shear on the undrained cyclic behavior of sandy soils has been long investigated by means of well-controlled laboratory tests, namely conventional triaxial testing (Lee et al., 1967; Vaid et al., 1983, Hyodo et al., 1991 and 1994; Yang and Sze, 2011; among others), or using simple shear devices, which can simulate field stress conditions expected during earthquakes more

[1] Graduate Student, Department of Civil Engineering, University of Tokyo
[2] Lecturer, Department of Civil and Natural Resources Engineering, University of Canterbury, Christchurch, New Zealand
[3] Associate Professor, Institute of Industrial Science, University of Tokyo

accurately than triaxial testing (Yoshimi et al., 1975; Vaid et al., 1979; Ishihara and Takatsu, 1977; Tatsuoka et al., 1982; Chiaro et al., 2012 and 2013). The major conclusion from these tests is that the initial static shear stress has a significant effect on the liquefaction resistance of sandy soils, in conjunction with the earthquake-induced cyclic shear stress, the soil relative density, confining pressure, among other factors. Furthermore, Yang and Sze (2011) showed that there are three different failure modes for sand under undrained triaxial cyclic loadings with initial static shear: flow-type failure, cyclic mobility and accumulated plastic strain. Among those, flow-type failure is the most critical since it is characterized by abrupt, runaway deformations without any warning signal. Similar failure modes have been also observed by Chiaro et al. (2012) on fully-saturated medium-dense (D_r = 44-50%) Toyoura sand specimens tested in a hollow cylinder torsional shear apparatus. However, there are still uncertainties in regard to the failure modes for very loose sand (D_r = 25-30%), i.e. liquefaction triggering mechanisms and consequent development of extremely large deformation.

Consequently, in this study, to gain a better understanding on the effects of initial static shear on large deformation behavior of very loose sand subjected to undrained cyclic loading, a series of torsional simple shear tests were carried out on hollow cylindrical specimens of Toyoura sand having a D_r =24-30% and subjected to single amplitude shear strain exceeding 50%.

STRESS CONDITIONS IN SLOPED GROUND DURING EARTHQUAKES

As schematically shown in Figure 1, before earthquake shaking, a soil element beneath sloped ground is subjected to an initial static shear stress (τ_{static}) induced by slope inclination conditions. During earthquake shaking, the soil element can experience partially reversed or non-reversed shear stress loading conditions, due to the superimposition of static shear stress with cyclic shear stress (τ_{cyclic}). Specifically, when $\tau_{static} < \tau_{cyclic}$, during each cycle of loading the shear stress changes within a maximum positive value τ_{max} (= $\tau_{static} + \tau_{cyclic}$) > 0 to a minimum negative value τ_{min} (= $\tau_{static} - \tau_{cyclic}$) < 0. This type of loading is known as reversal stress or two-way loading. On the other hand, when $\tau_{static} > \tau_{cyclic}$, the shear stress is always positive (i.e. $\tau_{max} > 0$ and $\tau_{min} > 0$). Consequently, non-reversal stress or one-way loading takes place (Yoshimi and Oh-oka, 1975; Hyodo et al., 1991; Towhata, 2008).

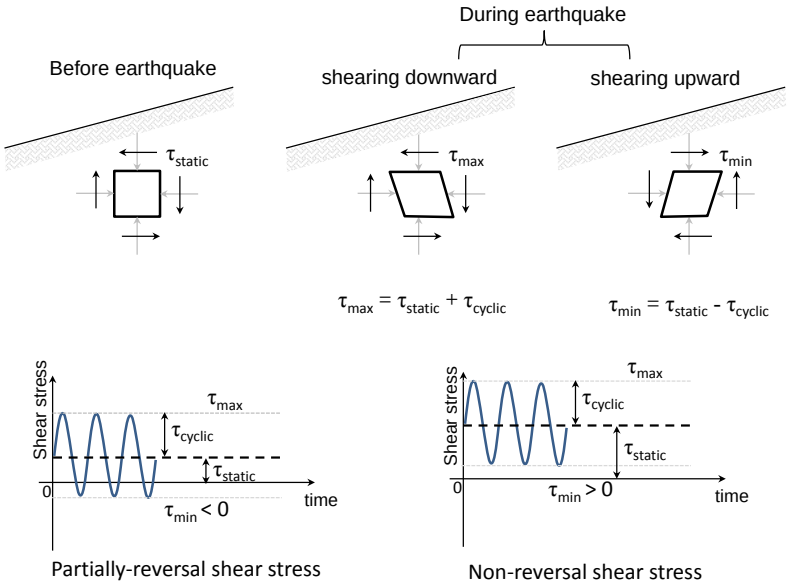

Figure 1. Stress conditions in sloped ground before and during earthquakes (after Chiaro et al., 2015)

TEST APPARATUS

Laboratory testing was carried out using the fully automated torsional apparatus shown in Figure 2, which has been developed by Kiyota et al. (2008) in the Institute of Industrial Science, University of Tokyo. Such a device is capable of achieving double amplitude shear strain levels exceeding 100% by using a belt-driven torsional loading system that is connected to an AC servo motor through electro-magnetic clutches and a series of reduction gears. Torque and axial load are measured by a two-component load cell, which is installed inside the pressure cell, having axial load and torque capacities of 8kN and 0.15kNm, respectively. Difference in pressure levels between the cell pressure and the pore water pressure, are measured by a high-capacity differential pressure transducer (HCDPT) with a capacity of over 600 kPa. A potentiometer with a wire and a pulley is employed to measure large torsional deformations. Specified shear stress amplitude are controlled by a computer, which monitors the outputs from the load cell, computes the shear stress to conduct the cyclic shear tests. The measured shear stress is corrected for the effects of the membrane force, as described by Chiaro et al. (2015).

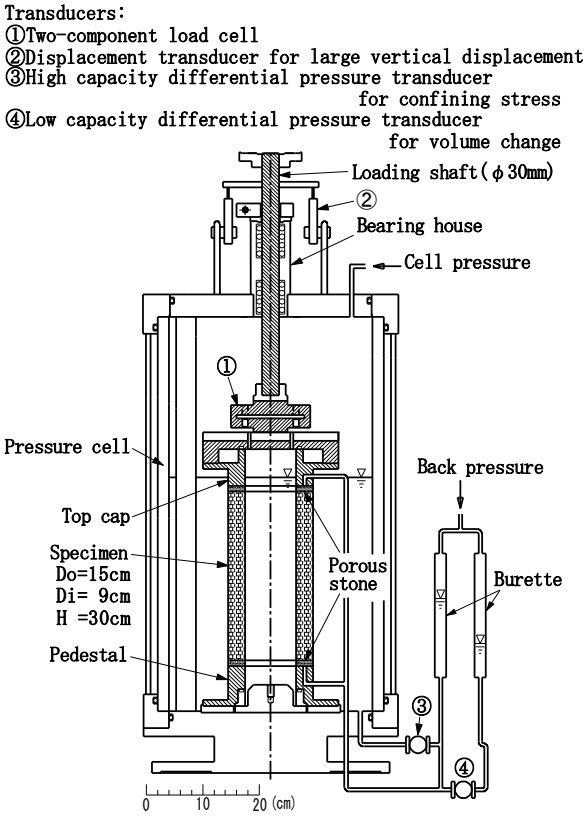

Figure 2. Torsional shear apparatus employed in this study (after Kiyota et al., 2008)

TEST PROCEDURE

All the tests were performed on Toyoura sand (see its index properties in Table1), which is a uniform sand with negligible fines content. Several medium-size hollow cylindrical specimens with dimension of 150 mm in outer diameter, 90 mm in inner diameter and 300 mm in height were prepared by air pluviation method at a relative density of 27 ± 3 %. After being saturated, the specimens were isotropically consolidated by increasing the effective stress state up to 100 kPa, with a back pressure of 200 kPa. Subsequently, a specific value of initial static shear (i.e. shear stress component induced by slope inclination) was applied by drained monotonic torsional shear loading. Finally, to replicate

seismic conditions, a constant-amplitude undrained cyclic torsional shear stress was applied at a shear strain rate of 0.5 %/min. The loading direction was reversed when the amplitude of shear stress, which was corrected for the effect of membrane force (Chiaro et al., 2015), reached the target value. During the process of undrained cyclic torsional loading the vertical displacement of the top cap was prevented with the aim to simulate as much as possible the simple shear condition that ground undergoes during horizontal excitation. To consider various combinations of initial static and cyclic shear stresses, tests were performed over a wide range of initial static shear varying from 0 to 25 kPa, while applying a cyclic shear stress of 16 kPa (see test detail in Table 2).

Table 1. Material index properties

Material	Specific gravity G_s	Minimum void ratio e_{min}	Maximum void ratio e_{max}	Mean Diameter D_{50} (mm)	Fines content F_C (%)
Toyoura sand	2.659	0. 608	0.951	0.16	0.1

Table 2. List of undrained cyclic torsional simple shear tests performed in this study

Test	Relative density D_r (%)	Shear stresses $\tau_{max,min} = \tau_{cyclic} \pm \tau_{static}$ (kPa)				Type of Loading
		τ_{cyclic}	τ_{static}	τ_{max}	τ_{min}	
No. 1	24.1	16	0	16	-16	Reversal
No. 2	25.7	16	5	21	-11	Reversal
No. 3	25.6	16	10	26	-6	Reversal
No. 4	29.8	16	15	31	-1	Reversal
No. 5	28.1	16	20	36	4	Non-Reversal
No. 6	28.9	16	25	41	9	Non-Reversal

TEST RESULTS AND DISCUSSION

Correction for membrane force

Koseki et al. (2005), among others, pointed out that in performing torsional shear tests on hollow cylindrical soil specimens, due to the presence of inner and outer membranes, the effect of membrane force on measured torsional shear stress cannot be neglected (i.e. to calculate the actual shear stress applied on soils, the total stress measured by load cell needs to be corrected from the apparent shear stress induced by presence of membrane, namely membrane force). Furthermore, membrane force becomes significantly important when shear strain reaches extremely large levels (Kiyota et al. 2008; Chiaro et al., 2012).

Usually, the membrane force is corrected based on the linear elasticity theory, which assumes cylindrical deformation of specimen. Accordingly, the theoretical apparent shear stress (τ_m) induced by the inner and the outer membranes can be evaluated as follows:

$$\tau_m = \frac{t_m E_m \left(r_o^3 + r_i^3\right)\theta}{\left(r_o^3 - r_i^3\right)H} \tag{1}$$

where

$$\theta = \frac{3\left(r_o^2 - r_i^2\right)H}{2\left(r_o^3 - r_i^3\right)}\gamma \tag{2}$$

where θ is the rotational angle of the top cap detected by external potentiometer; H is the height of the specimen; r_o and r_i are the outer and inner radii of the specimen; τ_m and E_m are, respectively, the thickness (= 0.3 mm) and the Young's modulus (= 1470 kPa; Tatsuoka et al., 1986) of the membrane.

However, as shown in Fig. 3, experimental evidences clearly show that at large shear strains, deformations of a hollow cylindrical sand specimen are not uniform along specimen height, as well as specimen shape is far from being perfectly cylindrical (Kiyota et al., 2010; Chiaro et al., 2013). Thus, in this study, the shear stress was corrected for the effect of membrane force by employing the empirical hyperbolic correlation between γ and τ_m, obtained by Chiaro et al. (2015) by means of monotonic and cyclic torsional shear tests carried out on two hollow cylindrical water specimens (Figure 3).

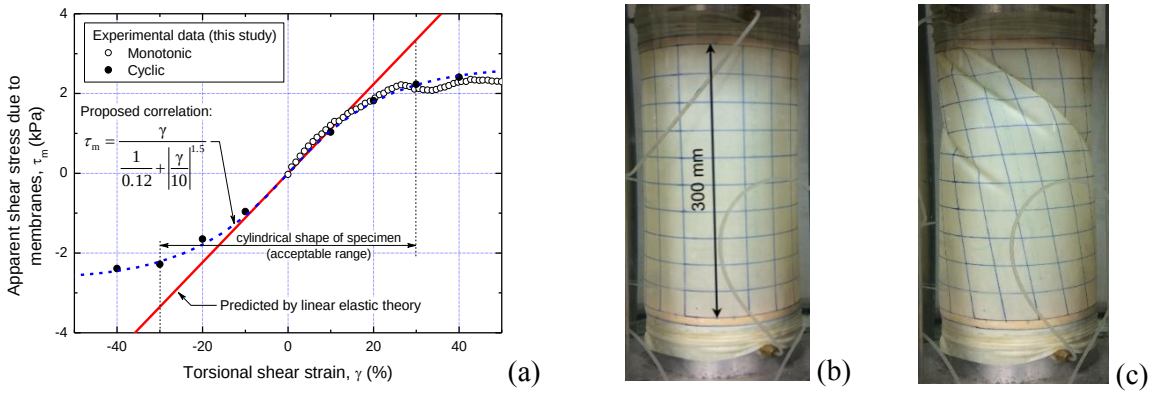

Figure 3. (a) Comparison between measured and calculated membrane force (adopted from Chiaro et al., 2015); (b) water specimen before monotonic shear test; and (c) water specimen deformation at $\gamma_{SA} \approx$ 25% during monotonic shear test

Undrained cyclic torsional shear behavior of very loose sand

Typical test results, in terms of effective stress paths and stress strain relationships, describing cyclic loading behavior of very loose Toyoura sand specimens subjected to different level of initial static shear stress and loading conditions are shown in Figure 4 through Figure 7.

Figures 4 and 5 show results of reversal stress Test No.1 and Test No.2, respectively. In these two tests, cyclic mobility was observed in the effective stress paths, where the effective stress recovered repeatedly after achieving the state of zero effective stress (i.e., full liquefaction). It was accompanied with a significant development of shear strain as evidenced by stress-strain relationships.

For Test No. 2, the specimen deformation at several states as numbered stage 1 through stage 4 is shown in Photo 1. At state 1, corresponding to a shear strain (γ) of about 7.5 %, the deformation was uniform throughout the specimen. At state 2 (γ = -10 %), although some wrinkles appeared on the outer membrane due to local drainage, the deformation was still rather uniform. At stage 3 (γ = -30 %), the outer membrane wrinkled more markedly at several locations. It looks as if the deformation of the specimen started to localize, in particular in the upper part of the specimen. At state 4 (γ = 80 %), the specimen was twisted extensively.

As shown in Figure 6, in the case of reversal stress loading Test No. 4 with $\tau_{cyclic} \cong \tau_{static}$, excessive pore water pressure developed rapidly, followed by extremely large deformation in just a few cycles of loading. It is noted that, this test results are very similar to those reported by Chiaro et al. (2012 and 2013) for the case of intermediate loading ($\tau_{cyclic} = \tau_{static}$).

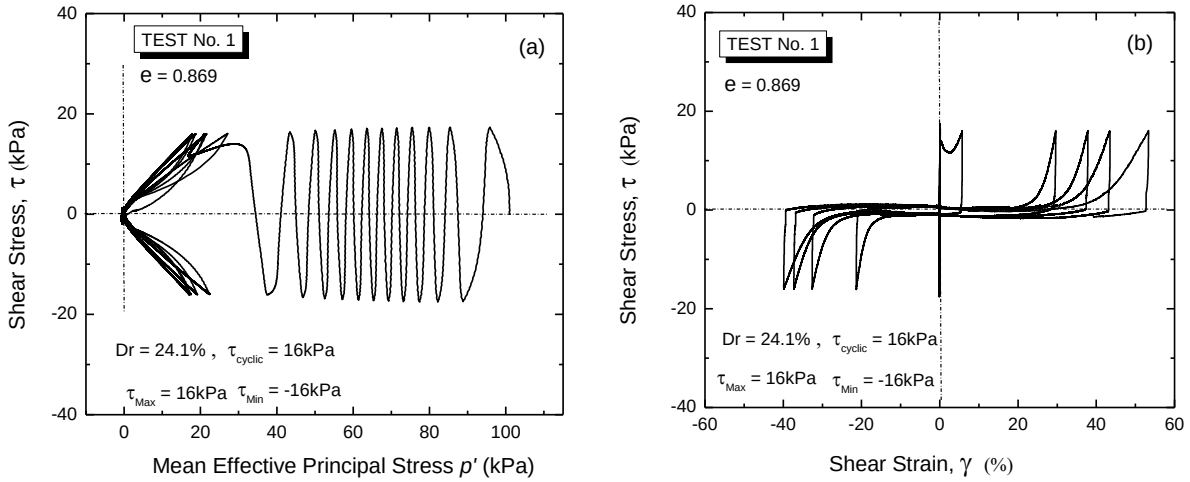

Figure 4: Test results for reversal stress Test No. 1 (τ_{static} = 0)

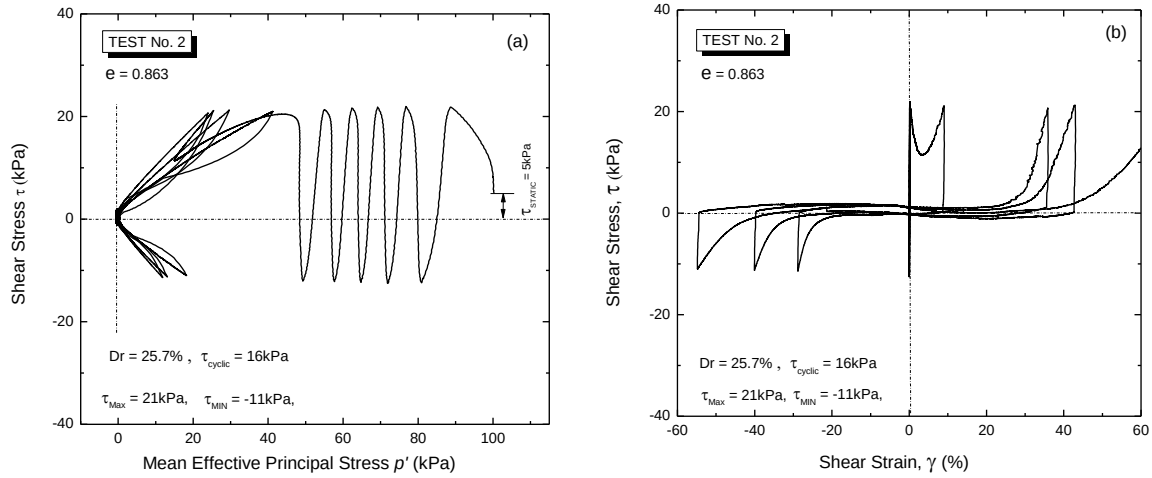

Figure 5: Test results for reversal stress Test No. 2 (τ_{static} = 5 kPa)

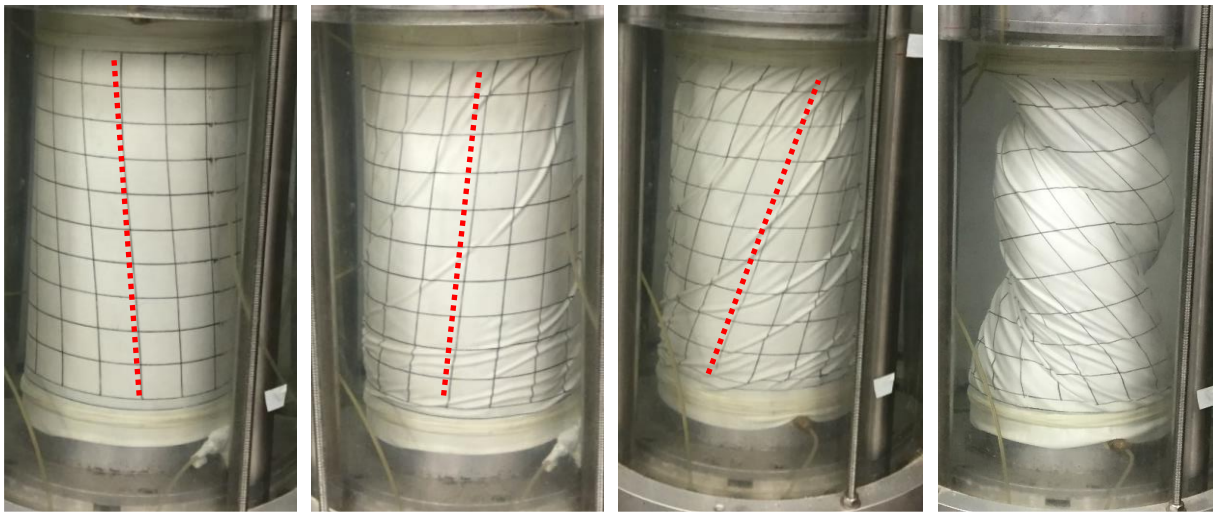

Stage 1 γ = 7.5% | Stage 2 γ = -10% | Stage 3 γ = -30% | Stage 4 γ = 80%

Photo 1: Specimen deformation observed for reversal stress Test No. 2 (τ_{static} = 5 kPa)

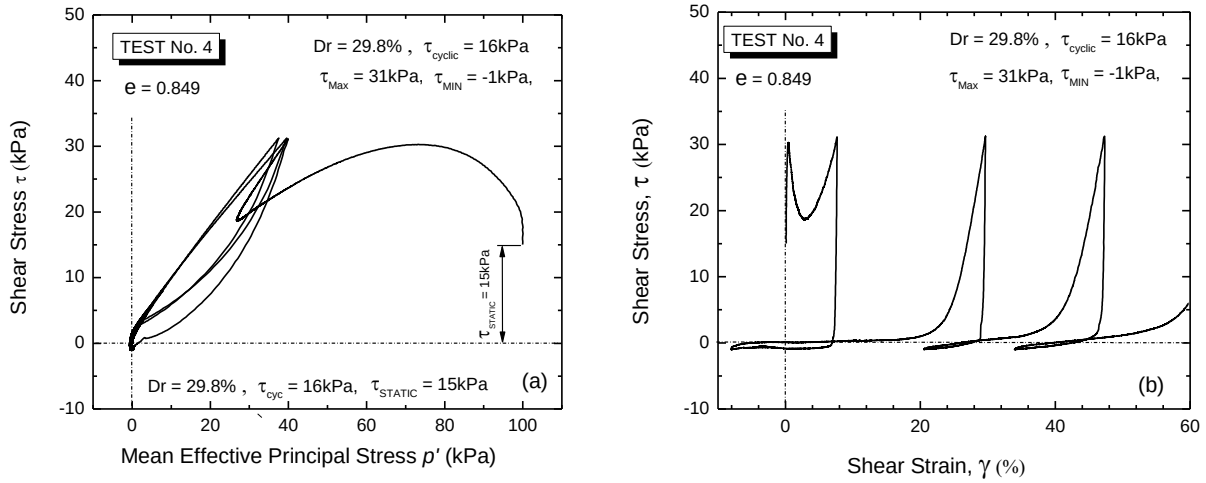

Figure 6: **Test results for reversal stress Test No. 4 (τ_{static} = 15 kPa)**

Figure 7 shows typical non-reversal loading test results (Test No. 5). In this case, the state of zero effective stress was not achieved even after applying 19 cycles of loading. Even though liquefaction did not occur, a large shear strain level exceeding 50 % was reached. Moreover, in this test, during the first cycle, relatively high shear strain level of 20% was achieved. It was then followed by a more progressive development of shear strain up to γ = 40%, after which a sudden development of shear strain took place probably due to formation of shear band(s) within the specimens. Specimen deformation for Test No.5 is shown in Photo 2. The specimen deformation is rather uniform up to stage 3 (γ = 40%), except for some wrinkles on the outer membrane.

The results of the above non-reversal loading test indicate that, when the combined shear stress cannot achieve the zero state, full liquefaction (i.e., the zero effective stress state) does not occur. However, this does not mean that sand is very resistant against seismic loading; in fact a significant magnitude of combined shear stress may cause failure as evidenced with the formation of shear band(s).

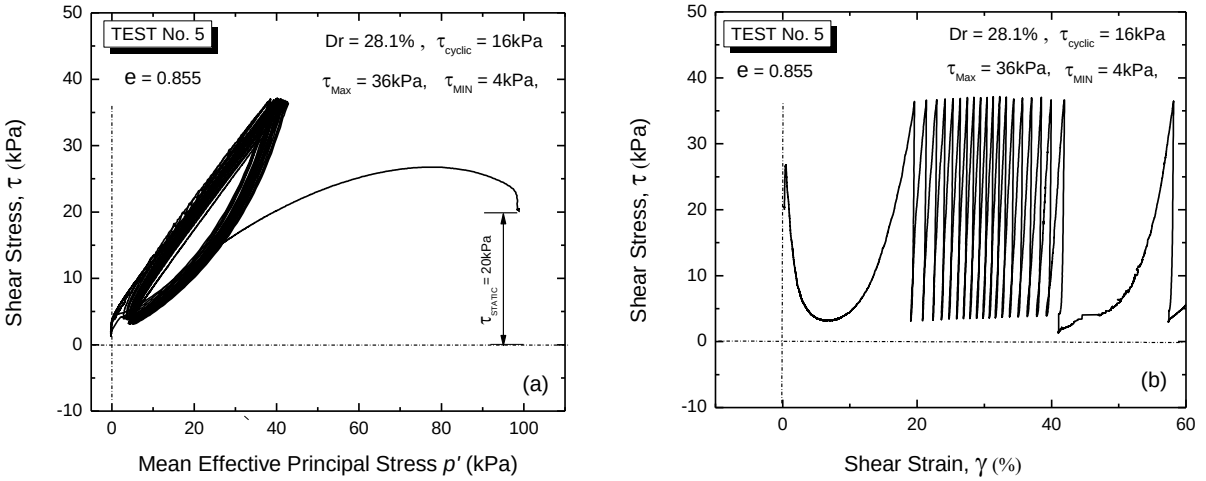

Figure 7: Test results for non-reversal stress Test No. 5 (τ_{static} = 20 kPa)

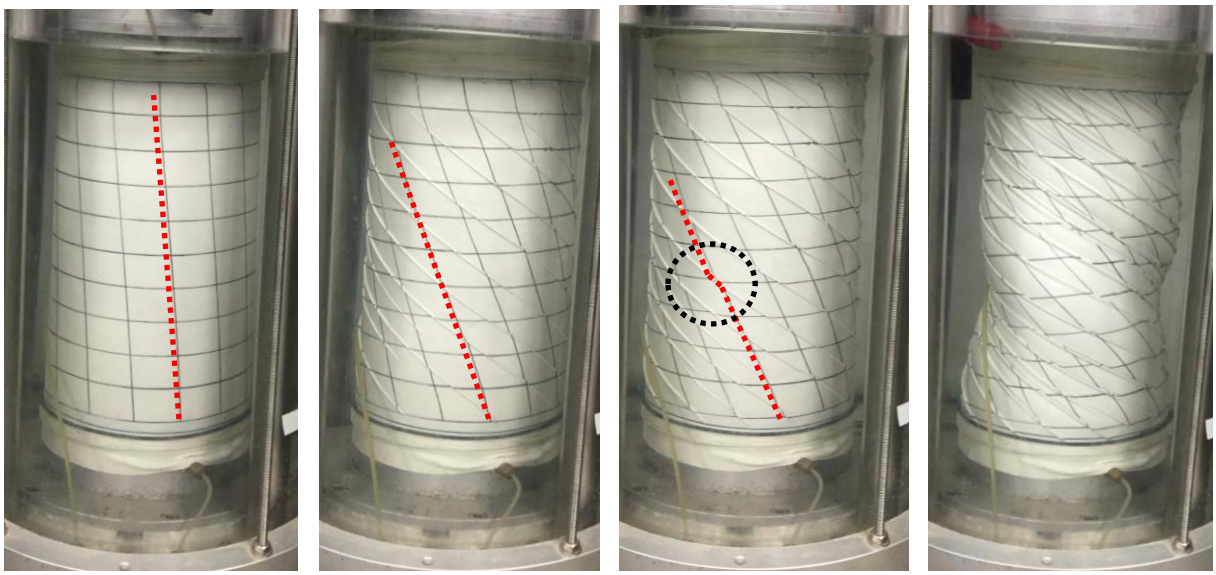

Stage 1 γ = 7.5% | Stage 2 γ = 30% | Stage 3 γ = 40% | Stage 4 γ = 80%

Photo 2: Specimen deformation observed for non-reversal stress Test No. 5 (τ_{static} = 20 kPa)

Resistance against extremely large cyclic strain accumulation

In case of level ground conditions, cyclic liquefaction resistance is expressed by cyclic stress ratio (CSR = τ_{cyclic}/p') required to develop a specific amount of deformation during cyclic loading (i.e., single or double amplitude shear strain). However, in case of sloped ground, due to the presence of initial static shear, it can be seen that SSR (= τ_{static}/p_0') is a more suitable parameter to describe the effects of initial static shear on the resistance to liquefaction of cyclic shear strain accumulation. Moreover, shear strain accumulation is usually more predominant in the direction were static shear is applied. Therefore, double amplitude shear strain (γ_{DA}) becomes unsymmetrical as described by Chiaro et al. (2012). Consequently, in order to have better understanding of liquefaction resistance against strain accumulation in case of initial static shear, Chiaro et al. (2012) suggested to use single amplitude shear strain (γ_{SA}) rather than γ_{DA} to evaluated liquefaction resistance as shown in Figure 8.

Torsional shear test conducted by Chiaro et al. (2012), on loose Toyoura sand (D_r = 44-50%) revealed that in the case of non-reversal loading ($\tau_{static} > \tau_{cyclic}$), Toyoura sand become more resistant against strain accumulation. Similar behavior was observed also in this study for the very loose Toyoura sand specimens (Figure 8a).

As shown in Figure 8a, comparison between test results presented by Chiaro et al. (2012) and those obtained in this study, allows for a better understanding about combined effects of relative density (D_r) and initial static shear on the liquefaction resistance of Toyoura sand. In general it can be seen that, despite the different level of density, sand behavior trend is reasonably similar. In fact, under reversal stress loading ($\tau_{static} < \tau_{cyclic}$), a drastic reduction in the liquefaction resistance is observed as level of initial static shear increase. However, under non-reversal stress ($\tau_{static} > \tau_{cyclic}$), cyclic strain accumulating resistance increases with the initial static shear increase. Moreover, it is clear that the loose sand is much weaker against liquefaction/cyclic strain accumulation.

Figure 8b compares resistance of very loose Toyoura sand for different level of strain accumulation i.e. 20%, 30% and 40%. Interestingly, it is noted that, under non-reversal stress loading, shear strain accumulation resistance is much larger for shear strain level larger than 20%. One of the possible explanations for such behavior is that very loose sand tends to contract during cyclic shearing and thus gain more frictional interlocking resistance.

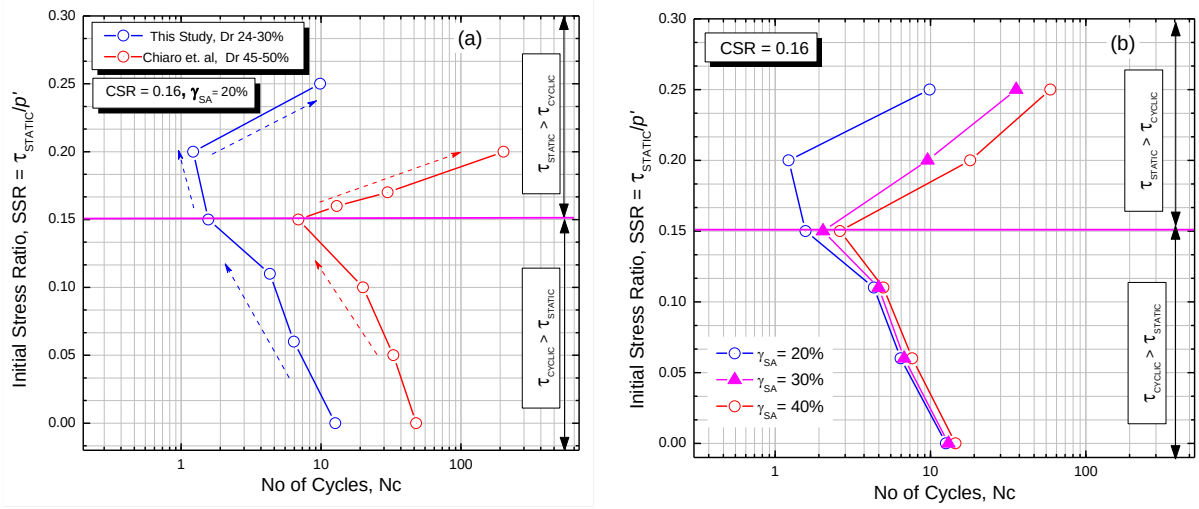

Figure 8: a) Cyclic strain accumulation for γ_{SA} = 20%, SSR vs Number of cycles b) Development of Shear strain vs Number of cycles during undrained cyclic torsional test

CONCLUSIONS

Soil beneath the sloping ground is always subjected to an initial driving shear stress prior seismic loading. In order to investigate the effect of static shear stress on the cyclic behavior of liquefied sand, a series of undrained cyclic torsional shear tests was conducted on saturated very loose Toyoura sand specimens (D_r = 24-30%) up to extremely large deformation. From the present study, analyses of test results revealed that:

a) By employing a modified torsional simple shear device, undrained cyclic torsional shear tests with initial static could be conducted on very loose Toyoura sand specimens up to single amplitude shear strain exceeding 50%;

b) Very loose Toyoura sand undergoing cyclic torsional shear stress behaved in two different ways depending on the value of combined shear stress ($\tau_{static} + \tau_{cyclic}$). In case of reversal loading, the sand easily liquefied and large deformation was developed while showing cyclic mobility. On the other hand, in case of non-reversal loading, liquefaction did not occur;

c) Both the effective stress paths and the stress-strain relationships were affected by the initial static shear stress level, in a similar way observed in previous studies carried out on medium dense specimens (D_r = 45-50%);

d) It the case of very loose sand, a decrease in liquefaction resistance was observed up to 20% shear strain during non-reversal loading;

e) In general shear strain accumulation resistance of very loose specimen is much smaller as compared with that of medium dense sand specimens.

REFERENCES

Chiaro, G., Kiyota, T. and Koseki, J. (2013): Strain localization of characteristics of loose saturated Toyoura sand in undrained cyclic torsional shear tests with initial static shear, *Soils and Foundations*, **53**(1): 23-34.

Chiaro, G., Kiyota, T., Pokhrel, R. M., Goda, K., Katagiri, T. and Sharma, K. (2015): Reconnaissance report on geotechnical and structural damage caused by the 2015 Gorkha Earthquake, Nepal, *Soils and Foundations*, **55**(5): 1030-1043.

Chiaro, G., Kiyota, T. and Miyamoto, H. (2015b): Large deformation properties of reconstituted Christchurch sand subjected to undrained cyclic torsional simple shear loading, *Proc. of the 2015 NZSEE Conference*, Apr. 10-12, Rotorua, New Zealand, 529-536.

Chiaro, G., Koseki, J. and Kiyota, T. (2015a): New insights into the failure mechanisms of liquefiable

sandy sloped ground during earthquakes, *Proc. of the 6th International Conference on Earthquake Geotechnical Engineering*, Nov. 1-4, Christchurch, New Zealand, CD-ROM, pp.8.

Chiaro, G., Koseki, J. Sato, T. (2012): Effects of initial static shear on liquefaction and large deformation properties of loose saturated Toyoura sand in undrained cyclic torsional shear tests, *Soil and Foundations*, **52**(3): 498–510.

Cubrinovski, M., Green, R.A., Allen, J., Ashford, S. A., Bowman, E., Bradley, B. A., Cox, B., Hutchinson, T. C., Kavazanjian, E., Orense, R. P., Pender, M., Quigley, M. and Wotherspoon, L. (2010): Geotechnical reconnaissance of the 2010 Darfield (Canterbury) Earthquake, *Bulletin of the New Zealand Society of Earthquake Engineering*, **42**(4): 243-320.

Cubrinovski, M., Bray, J. D., Taylor, M., Giorgini, S., Bradley, B. A., Wotherspoon, L. and Zupan, J. (2011): Soil liquefaction effects in the Central Business Districts during the February 2011 Christchurch Earthquake, *Seismological Research Letters*, **82**(6): 893-904.

Hamada, M., O'Rourke, T. D. and Yoshida, N. (1994): Liquefaction-induced large ground displacement, Performance of Ground and Soil Structures during Earthquakes, 13th ICSMFE, JGS, 93-108.

Hyodo, M., Murata, H., Yasufuku, N. and Fujii, T. (1991): Undrained cyclic shear strength and residual shear strain of saturated sand by cyclic triaxial tests, *Soils and Foundations*, **31**(3): 60-76.

Hyodo, M., Tanimizu, H., Yasufuku, N. and Murata, H. (1994): Undrained cyclic and monotonic triaxial behavior of saturated loose sand, *Soils and Foundations*, **34**(1): 19-32.

Ishihara, K., and Takatsu, H. (1977): Pore pressure buildup in initially sheared sand subjected to irregular excitation, *Proceedings of the 6th World Conference on Earthquake Engineering, New Delhi, India*, 2163-2168.

Kiyota, T., Kyokawa, H. and Konagai, K. (2011): Geo-disaster report on the 2011 Tohoku-Pacific Coast Earthquake, *Bulletin of Earthquake Resistant Structure Research Center*, 44: 17-27.

Kiyota, T., Sato, T., Koseki, J., and Mohammad, A. (2008): Behavior of liquefied sands under extremely large strain levels in cyclic torsional shear tests, *Soils and Foundations*, **48**(5), 727-739.

Kiyota, T., Koseki, J. and Sato, T. (2010): Comparison of liquefaction-induced ground deformation between results from undrained cyclic torsional shear tests and observations from previous model tests and case studies, *Soils and Foundations*, **50**(3): 421-429.

Koseki, J., Yoshida, T. and Sato, T. (2005): Liquefaction properties of Toyoura sand in cyclic torsional shear tests under low confining stress, *Soils and Foundations*, **45**(5), 103-113.

Lee, K. L., and Seed, H. B. (1967): Dynamic strength of anisotropically consolidated sand, *Journal of the Soil Mechanics and Foundations Division, ASCE*, **93**(SM5): 169-190.

Seed, H. B., Idriss, I. M., Lee, K. L. and Makadisi, F.I. (1975): Dynamic analysis of the slide in the Lower San Fernando Dam during the Earthquake of February 9, 1971, *Journal of the Geotechnical Engineering Division*, ASCE, **GT9**: 889-911.

Tatsuoka, F., Muramatsu, M. and Sasaki, T. (1982): Cyclic undrained stress-strain behavior of dense sand by torsional simple shear test, *Soils and Foundations*, **22**(2), 55-69.

Tatsuoka, F., Sonoda, S., Hara, K., Fukushima S. and Pradhan, T. B. S. (1986). Failure and deformation of sand in torsional shear, *Soils and Foundations*, **26**(4): 79-97.

Towhata, I. (2008): *Geotechnical Earthquake Engineering*, Springer.

Vaid, Y. P. and Finn, W.D.L. (1979): Static shear and liquefaction potential, *Journal of Geotechnical Engineering Division, ASCE*, **105**(GT10): 1233-1246.

Vaid, Y. P. and Chern, T. C. (1983): Effect of static shear on resistance to liquefaction, *Soils and Foundations*, **23**(1): 47-60.

Yang, J. and Sze, Y. (2011): Cyclic behavior and resistance of saturated sand under non-symmetrical loading conditions, *Geotechnique*, **61**(1): 59-73.

Yoshimi, Y. and Oh-oka, H. (1975): Influence of degree of shear stress reversal on the liquefaction potential of saturated sand, *Soils and Foundations*, **15**(3): 27-40.